

Characterization of a welding wire by rotating-beam fatigue test

Caracterização em fadiga por flexão rotativa de fios de arame de solda

Ingrid Ariani Belineli Barbosa¹, Heide Heloise Bernardi¹, William Marcos Muniz Menezes¹

ABSTRACT

The objective of this work was to determine the fatigue life of wire materials by rotary bending and to identify parameters of mechanical loading and deformation associated with the characteristics of the rupture generated by fatigue to prevent failures. An AWS A5.18 welding wire with diameter 0.80 mm was used as the specimen. The welding wire specimens were subjected to an average rotation of 611.3 rpm with a bending radius of 80 mm. The results show that the welding wire supports around 10,000 cycles until its fracture, and SEM image analysis indicates a combined fracture of failure and ductile fractures.

Keywords: Fatigue, Rotating beam, Welding wire.

RESUMO

O objetivo deste trabalho foi determinar a vida em fadiga de materiais na forma de fios sob esforços de flexão rotativa e também identificar parâmetros de carregamento mecânico e deformação associados às características da ruptura gerada pela fadiga, a fim de se estabelecer procedimentos para prevenção dessas falhas. Utilizou-se como material de teste um arame de solda da classe AWS A5.18 com diâmetro de 0,80 mm. Os corpos de prova do fio foram submetidos à rotação média de 611,3 rpm com um raio de flexão de 80 mm. Os resultados mostram que o arame de solda suporta em torno de 10.000 ciclos até a fratura, e as análises fractográficas indicaram uma fratura combinada de falha por fadiga e fratura dúctil.

Palavras-chave: Fadiga, Flexão rotativa, Arame de solda.

¹Faculdade de Tecnologia de São José dos Campos – FATEC Professor Jessen Vidal – São José dos Campos/SP – Brazil.

Correspondence author: Ingrid Ariani Belineli Barbosa | Faculdade de Tecnologia de São José dos Campos – FATEC Professor Jessen Vidal | Av. Cesare Monsueto Giulio Lattes, 1350 | CEP 12.247-014 – São José dos Campos/SP – Brazil | E-mail: ariabelineli@gmail.com

Received: Feb. 16, 2018 | **Accepted:** Mar. 21, 2018

INTRODUCTION

The study of the phenomenon of material fracture by cyclic mechanical stresses has a special relevance in the wire spinning, given the processes of manufacture and use of metallic wires, which invariably impose on the movement of wire between pulleys or even its displacement by sinuous guides and machines. Siderurgical Gerdau produced the AWS A5.18 welding wire studied in this work. The wire is indicated for semiautomatic, mechanized, and robot welding and it is widely used in boilers, automotive parts, road equipment, mechanical construction, and agricultural machinery¹. This welding wire is used in MIG/MAG (Metal Inert/Active Gas) welding, and during its usage the wire does not significantly undergo mechanical stress. However, it is important to know the mechanical characteristics of this material for better control of the forming process of this wire.

Cyclic mechanical loading causes fatigue failure of metallic materials and generates progressive and localized structural damage. The stress applied to the material during the fatigue process is lower than its yield strength. Although fatigue can be studied under conditions of pure stress forces, in this work the rotary bending tests were used to evaluate the fatigue strength of the material². The fatigue life is determined by the total number of cycles the material can resist until its rupture and/or failure³.

Materials submitted to mechanical fatigue have the following morphology in their fracture: (a) loading cycle forms beach marks, (b) one applied loading cycle forms each striation, and (c) dimples, also known as microvoids, initiate the crack formation^{2,3}.

The present paper shows the results of a mechanical evaluation of a welding wire by rotating-beam fatigue test. Thereafter, a fractographic analysis was performed using a scanning electron microscopy (SEM).

EXPERIMENTAL

Material

In this work, an AWS A5.18 ER70S-6 welding wire, with a nominal diameter of 0.80 mm and 400 MPa yield strength, whose chemical composition is shown in Table 1, was studied¹. The welding wire studied is also a low-carbon steel (less than 0.25% wt. carbon) subjected to normalizing, wire drawing, and electro-galvanizing treatment.

According to the Eq. 1 by the International Institute of Welding (IIW)⁴, the carbon equivalent (C_{eq}) of an AWS A5.18 ER70S-6 welding wire corresponds to 0.567. The C_{eq} (% wt._{max}) was calculated using the information from Table 1. The C_{eq} is associated to weldability, the lower the carbon equivalent, the lower the probability of obtaining a second stage precipitation

(carbide) or martensitic microstructure and, consequently, the better the weldability of the steel ($0.40 \leq C_{eq} \leq 0.60$ medium weldability). In the welding, it is important to know the chemical composition of the base material to select the correct preheating temperature⁵. Two major factors are required to determine the preheating temperature, such as the carbon equivalent and the alloy content of the material. If the carbon equivalent of the material is higher, it requires a higher preheating temperature⁶.

$$C_{eq} = C + \frac{Mn}{6} + \frac{(Cr + Mo + V)}{5} + \frac{(Ni + Cu)}{15} \quad (1)$$

Rotating-Beam Fatigue Test

A machine called ROTATFLEX 180, developed by Menezes^{7,8}, performed the rotating-beam fatigue test. The length of the specimen cut was 394 ± 7 mm, which was adequate to fix the wire in the rotating mandrel of the machine, and sufficient to obtain a semicircle curve. All specimens were attached to the rotating-beam fatigue-test machine using a curvature radius of 80 mm, resulting in the strain amplitudes (ϵ_s) of 0.5%, which means maximum strain in tension or compression on the outer surface of the bent wire. The rotational speeds were 611 ± 6.2 rpm.

Four samples were tested and the tests were carried out at room temperature. The samples were tested until the occurrence of wire failure. Figure 1 shows the schematic drawing of the fatigue machine used in the present investigation.

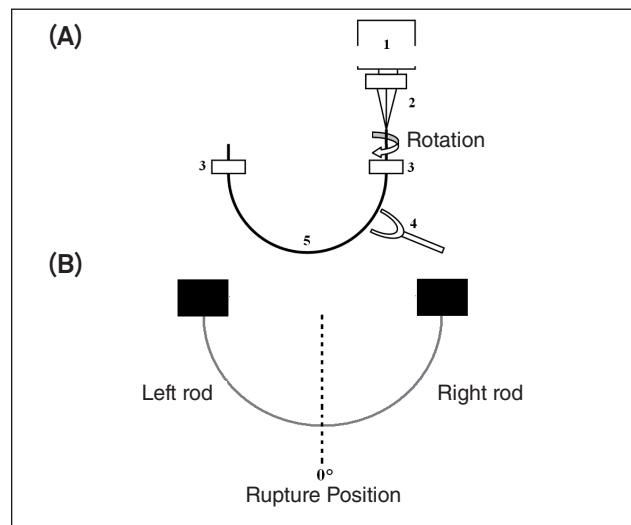


Figure 1: Schematic drawing of: (A) the ROTATFLEX 180 machine indicating (1) the motor, (2) the mandrel to fix the specimen, (3) the specimen support bearings, (4) the feeler gage that identifies sample rupture, and (5) the wire sample positioned in flexion⁸; and (B) mechanical test parameters.

Table 1: Chemical Composition of AWS A5.18 welding wire¹.

Elements (wt. %)	C	Si	Mn	S	P	Cu	Ni	Cr	Mo	V
% Min.	0.06	0.8	1.4	-	-	-	-	-	-	-
% Max.	0.15	1.15	1.85	0.035	0.025	0.5	0.15	0.15	0.15	0.03

Fractography

The fractographic of the specimens were imaged using a VEGA3 TESCAN scanning electron microscope (SEM) operating at 25 kV.

RESULTS AND DISCUSSION

Strain Calculations

The fatigue life of wire materials by rotary bending is determined by the number of stress cycles, the wire diameter (d), the rotational speed of the wire (ω), the bending radius of the wire arc of curvature (R), and strain (ϵ). As for the wire strain, in relation to cyclic rotary bending condition, ϵ_{ac} was considered the maximum deformation in compression, and ϵ_{at} as the maximum deformation in tensile. For this work, it was also considered that the effects of fatigue and hardening were the same for tensile and compression deformation due to the similar nature of these phenomena in small deformations. Thus, it was denominated both ϵ_{ac} and ϵ_{at} as ϵ_a .

The strain amplitudes (ϵ_e) were calculated according to Eq. 2 considering the neutral surface in the center of the wire as longitudinal⁷. For the calculation, the diameter used was 0.80 mm, and the bending radius was 80 mm. As a result, $\epsilon_a = 0.50\%$.

$$\epsilon_a = \frac{d}{2R} \times 100\% = \frac{0.80}{2 \times 80} \times 100\% = 0.50\% \quad (2)$$

The calculation of the maximum strain in the elastic condition (ϵ_e), according to Eq. 3, considered the following material parameters: yield strength (σ_y) of 400 MPa and Young's modulus (E) of 210 GPa. The result $\epsilon_e = 0.19\%$ was obtained.

$$\epsilon_e = \frac{\sigma_e}{E} = \frac{400}{210000} = 0.0019 = 0.19\% \quad (3)$$

The strain is directly proportional to the wire diameter, as shown in Eq. 2. Therefore, the circular section in the center of the wire, which is relative to 38% (0.38 d) of wire diameter, was subjected to elastic strain cycles, consequently fatigue cycles. On the other hand, the cross-section that corresponded to the outer circle was subjected to a strain greater than 0.19%, suffering hardening (Fig. 2). In other words, the strain distribution occurred from the center to the end of the wire surface. It is described as (A) in the center of the wire the strain was negligible or even null due to the bending, (B) from the center of the wire up to 0.38 d occurring cycling under elastic strain, that is fatigue, and (c) from the region 0.38 d of the wire to its surface, underwent to elasto-plastic strain and consequently hardening.

If $\epsilon_e = 0.19\%$ and $\epsilon_a = 0.50\%$, the welding wire suffered purely elastic strain in the central region (0.38 d) and elasto-plastic strain ranging from 0.19% to 0.50% on the wire surface, occurring different failure mechanisms in both regions.

For the wire studied in this work, it is possible to calculate (Eq. 4) the diameter from the region that suffered elastic strain considering a bending radius (R) of 80 mm and a maximum strain in the elastic condition (ϵ_e) of 0.0019 (from Eq. 3). As a result $d = 0.304$ mm, which represents the region that suffered elastic strain.

$$\epsilon_e = \frac{d}{2R} \rightarrow 0.0019 = \frac{d}{2 \times 80} \rightarrow d = 0.304 \text{ mm} \quad (4)$$

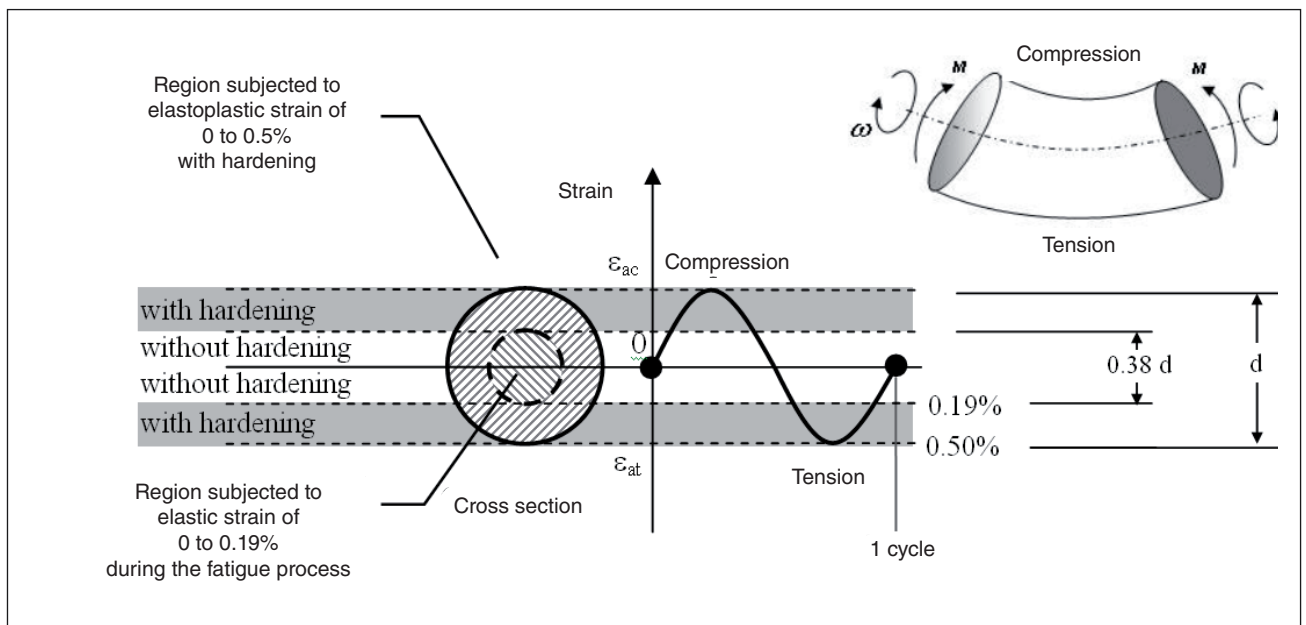


Figure 2: Wire strain according to cross-section area.

Rotary-Bending Fatigue

Table 2 shows the results of the rotating-beam fatigue-test for the welding wire specimens. The four specimens studied averaged 10.4×10^3 cycles until failure, and with a mean rotational speed of 611 rpm, for an average period of 17 min.

Table 2: Results of the rotating-beam fatigue test performed in welding wire specimens.

Variables	Sample 1	Sample 2	Sample 3	Sample 4
Number of cycles (Nf)	9599	10747	10177	10903
Time to failure (min)	15	17	17	18
Rotation speed (rpm)	615	618	606	606
Length of right rod after failure (mm)	177	195	133	183
Failure position (degree)	3°	3°	2°	3°

Fractography

Based on the fractographic analysis and the calculations obtained, a combined fracture surface was observed: fatigue fracture and ductile fracture. During the fatigue process, the edges of the wire surface ($\epsilon_a = 0.5\%$) are subjected to a plastic strain and hardening, resulting in favorable conditions for crack initiation. Figure 3a shows the crack propagation, and the white circle corresponds to the region that suffered elastic strain ($d = 0.304$ mm). The cracks propagation occurs towards the center of the wire in the elastic deformation region ($\epsilon_a = 0$). The cracks propagation begins at the fracture surface (Fig. 3b) of the wire and occurs from maximum strain amplitude (cylindrical surface) to minimum strain amplitude (zero). The center of the wire corresponds to the neutral axis of the rotary-bending fatigue⁷.

With cyclic loading, a crack will begin to form at the region of greatest stress concentration after some critical number of cycles. The crack will propagate and after a certain distance, the cross section can no longer support the loads, and the final rupture occurs. In general, fatigue failures proceed as follows: (A) cyclic plastic deformation before crack initiation, (B) initiation and cracks propagation, and (C) final rupture⁹.

Figure 4 shows the combined fracture resulted in contrasting characteristics between the edge of the surface (origin of fracture) and the center of the wire (end fracture). On the surface of the wire, where hardening occurs, it was observed a fracture with characteristics of a ductile fracture (region A, Fig. 4a). The fracture surface, where the crack initiation occurs, tends to be smooth (Fig. 4b)³. At the surface edge, the fracture morphology is related to a complete fatigue, whereas, in the center of the wire is related to a fracture without fatigue (ductile fracture). The ductile fracture occurs almost instantaneously when the minimum rupture tension is achieved due to the reduction of the section area (region B, Fig. 4a).

In the region corresponding to ductile fracture, it is observed a rough and fibrous surface and the presence of dimples, which are characteristics of a ductile fracture (Fig. 4b). Dimples are the result of the micro-stretching of the grains until their rupture. Consequently, the fracture is preceded by an energy accumulation by plastic strain. In other words, the presence of dimples indicates that a ductile fracture has occurred in the material.

The type of loading the component has experienced during its fracture determines the shape of the dimples produced, and the orientation of the dimples reveals the direction of crack extension. Equiaxed dimples are formed under conditions of uniform plastic strain in the direction of applied tensile stress, typically produced under conditions of tensile overload. On the other hand, elongated shaped dimples result from nonuniform plastic strain conditions, such as bending. These dimples are

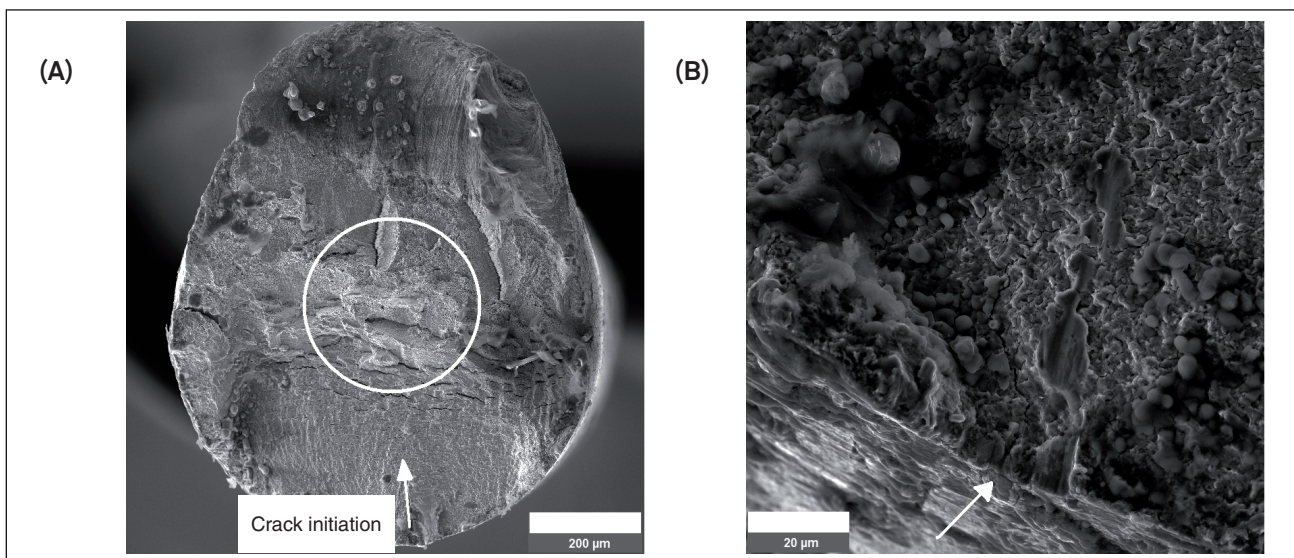


Figure 3: Wire and fracture surface showing: (A) nucleation and crack propagation, and (B) detailed view of crack initiation (SEM-SE).

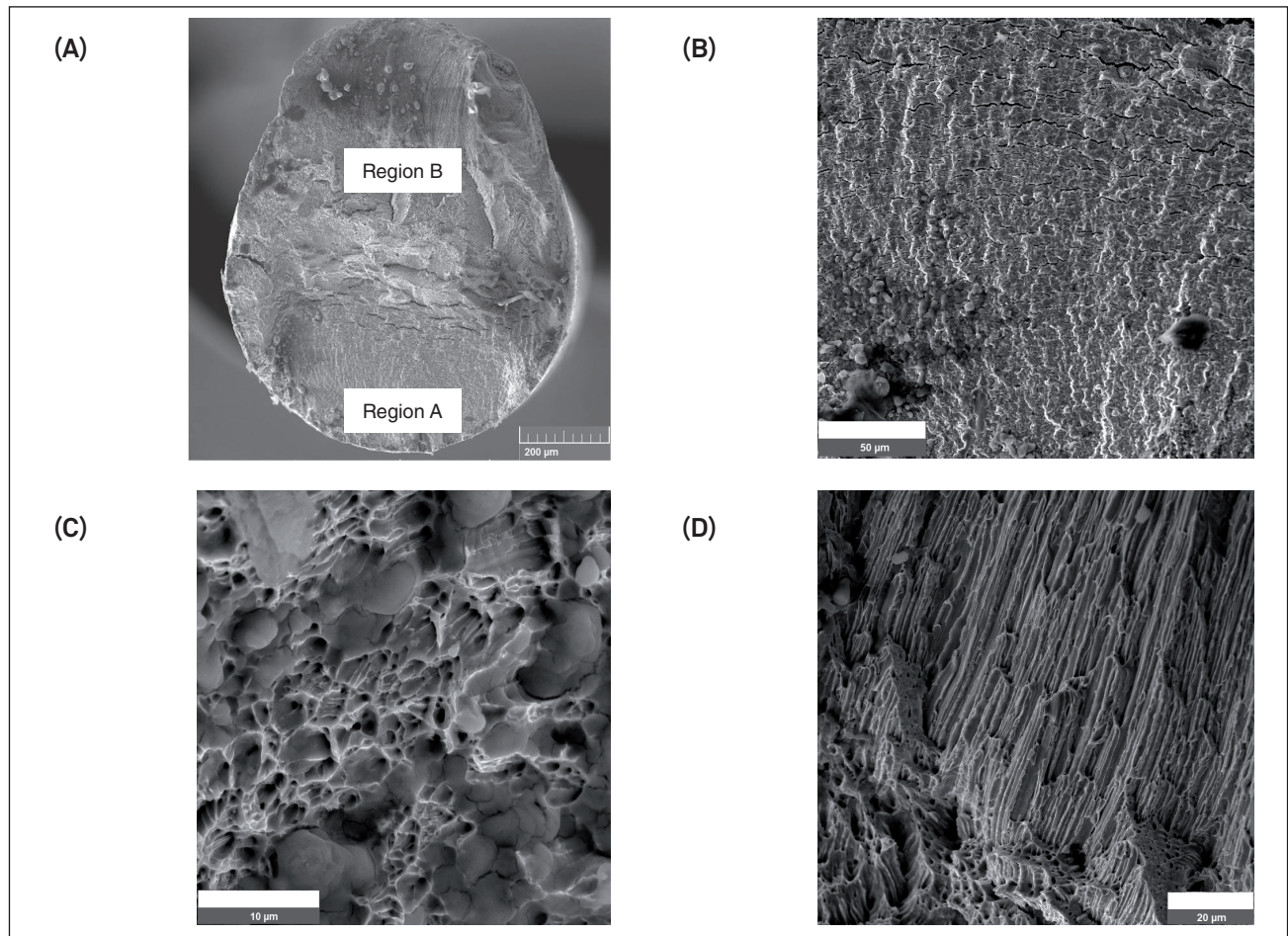


Figure 4: Fractography of welding showing: (A) macrograph of the fracture surface; (B) detail view of the region A; (C) the presence of equiaxed dimples, and (D) the presence of elongated dimples (SEM-SE).

elongated in the direction of crack extension and reveal the origin of the fracture⁹. Figures 4c and 4d show equiaxed and elongated dimples, respectively.

CONCLUSION

The rotating beam fatigue test performed in four welding wire specimens AWS A5.18 type ER705-6 demonstrated that the fracture has combined failure patterns: ductile fracture and fatigue fracture. However, due to the hardening that occurred on the surface of the material, the fracture had a brittle fracture aspect at the edge of the wire. Although it has a brittle fracture aspect, it is a ductile fracture with a progressive development generated by hardening in radial direction.

ACKNOWLEDGMENTS

The authors are thankful to ITA (Instituto Tecnológico de Aeronáutica) for the conventional SEM images and to FAPESP by financial support in the IV CIMATech (2017/13959-5).

REFERENCES

1. GERDAU. Arames para Solda [internet]. São Paulo: Gerdau; 2017. [Cited 2017 Aug. 8]. Available from: <https://www.gerdau.com/br/pt/productsservices/products/Document%20Gallery/catalogo-arames-para-solda.pdf>
2. Askeland DR, Wright WJ. Ciência e engenharia dos materiais. 3 ed. São Paulo: Cengage Learning; 2014.
3. Dieter GE. Metalurgia Mecânica. 2 ed. Rio de Janeiro: Editora Guanabara Dois; 1981.
4. Olson DL, Siewert TA, Liu S, Edwards GR, editors. ASM Handbook: welding, brazing and soldering. v. 6. Novoly: ASM International; 1993.
5. ESAB. Technical Handbook Submerged Arc Welding [internet]. ESAB; 2016. [Cited 2018 Jan. 27]. Available from: <http://assets.esab.com/asset-bank/assetfile/12295.pdf>
6. Fortes C, Araújo W. Apostila de metalurgia da soldagem [internet]. Contagem: ESAB; 2005. [Cited 2018 Jan. 17]. Available from: <http://www.esab.com.br/br/pt/education/apostilas/upload/apostilametalurgiasoldagem.pdf>
7. Menezes WMM. Influência do teor de carbono e oxigênio sobre a vida em fadiga por flexão rotativa de fios de ligas NiTi com Efeito

- Memória de Forma [PhD Thesis]. São José dos Campos: Instituto Tecnológico de Aeronáutica; 2013.
8. Menezes WMM, Matheus TCU, Otubo J. Projeto, fabricação e qualificação de equipamento para flexão rotativa de fios superelásticos de NiTi em ensaios de fadiga. *Tecnologia em Metalurgia, Materiais e Mineração*. 2014;11(1):14-21. <http://dx.doi.org/10.4322/tmm.2014.005>
9. Mills K, editor. *ASM Handbook: fractography*. v. 12. Novelty: ASM International; 1987.